SCIENCE CHINA
Life Sciences

THEMATIC ISSUE: Stem cells and regenerative medicine in China
• RESEARCH PAPER •

February 2014 Vol.57 No.2: 221–231
doi: 10.1007/s11427-014-4609-2

Investigating design principles of micropatterned encapsulation systems containing high-density microtissue arrays

JIANG LiYang[1], LIU JiaYing[1], WANG Kai[1], GU Xi[1] & LUO Ying[1,2*]

[1]*Department of Biomedical Engineering, College of Engineering, Peking University, Beijing 100871, China;*
[2]*National Engineering Laboratory for Regenerative and Implantable Medical Devices, Guangzhou 510663, China*

Received August 20, 2013; accepted October 12, 2013; published online January 15, 2014

Immunoisolation is an important strategy to protect transplanted cells from rejection by the host immune system. Recently, microfabrication techniques have been used to create hydrogel membranes to encapsulate microtissue in an arrayed organization. The method illustrates a new macroencapsulation paradigm that may allow transplantation of a large number of cells with microscale spatial control, while maintaining an encapsulation device that is easily maneuverable and remaining integrated following transplantation. This study aims to investigate the design principles that relate to the translational application of micropatterned encapsulation membranes, namely, the control over the transplantation density/quantity of arrayed microtissues and the fidelity of pre-formed microtissues to micropatterns. Agarose hydrogel membranes with microwell patterns were used as a model encapsulation system to exemplify these principles. Our results show that high-density micropatterns can be generated in hydrogel membranes, which can potentially maximize the percentage volume of cellular content and thereby the transplantation efficiency of the encapsulation device. Direct seeding of microtissues demonstrates that microwell structures can efficiently position and organize pre-formed microtissues, suggesting the capability of micropatterned devices for manipulation of cellular transplants at multicellular or tissue levels. Detailed theoretical analysis was performed to provide insights into the relationship between micropatterns and the transplantation capacity of membrane-based encapsulation. Our study lays the ground for developing new macroencapsulation systems with microscale cellular/tissue patterns for regenerative transplantation.

hydrogel, micropattern, array, multi-cellular spheroids, macroencapsulation

Citation: Jiang LY, Liu JY, Wang K, Gu X, Luo Y. Investigating design principles of micropatterned encapsulation systems containing high-density microtissue arrays. Sci China Life Sci, 2014, 57: 221−231, doi: 10.1007/s11427-014-4609-2

Since the early 1950s, immunoisolation devices have been investigated for encapsulating living cells in semi-permeable polymeric membranes to shield them from attack from the immune system following therapeutic cell transplantation [1,2]. Previous studies were performed for treatment of various types of tissue/organ disorders, including diabetes [3], hypothyroid [4], kidney/liver failure [5,6], and central nerves system diseases [7]. Among these studies, the immunoisolation of allogeneic or xenogenic islets were intensively examined for producing an artificial pancreas that does not require immunosuppression [8−10]. In recent years, with rapid developments in stem cell research and differentiation protocols that can provide cell sources for various tissues [11−13], the need for immunoisolation devices has grown even greater for regenerative therapy.

There generally exist micro- or macro-encapsulation devices for immunoisolation [14,15]. In microencapsulation, hydrated gel networks form a thin layer on the surface of individual microtissues. By contrast, the macroencapsulation devices are typically pre-fabricated and provide reser-

*Corresponding author (email: ying.luo@pku.edu.cn)

voirs large enough to constrain all microtissues required for transplantation. Typically, macroencapsulation devices are polymeric membrane-based, in the form of planar sheets or hollow fibers [16–20]. Because of their convenient maneuverability, one distinct advantage that macroencapsulation devices can offer is that the transplanted cells are totally retrievable or replaceable in the event of post-operative complications. Macroencapsulation devices therefore hold promise to provide off-the-shelf products for clinical use. Despite the feasibility and effectiveness shown in animal models, the translation of macroencapsulation devices into therapeutic products has so far been limited. This is mainly due to the inability of the devices to maintain efficient cell viability that ensures satisfactory therapeutic outcome, and the associated reasons are quite complex. Notably, fibrotic tissues resulting from the foreign-body reaction may affect nutrient exchange across the membrane. It is also noted that the macroencapsulated microtissues are randomly distributed, and the lack of spatial control may lead to clumping of cells and a risk of inducing tissue necrosis. In addition, the transplantation capacity of the device may be prohibitively insufficient; the volume of the device required to contain enough cellular content for treatment can be too large to be implanted in the body.

Recently, microfabrication techniques have been applied to create definable microstructures in hydrogel membranes [21–24]. In particular, hydrogel substrates patterned with microwells and microgrooves fabricated by micromolding processes enable the aggregation of cells with precise control of size, spacing and shape at the micro-level. The micromolding technique has been used to generate encapsulation sheets through gelling alginates *in situ* to embed pre-assembled cell-spheroidal arrays [25,26]. In another study, collagen-alginate hydrogels containing arrayed islet cells were tested in a diabetic mouse model, with the effective control of glucose levels over a 4-week period [27]. Therefore, micropatterned encapsulation systems (MESs) present a new type of macroencapsulation device. Despite this, major hurdles remain to be overcome before MES can be used for cell/tissue transplantation. Herein, we propose to examine the several issues regarding the design of MES. First, we will investigate whether micropatterns can improve microtissue density and whether the micropattern design can affect the transplantation capacity of the device. Second, given that pre-isolated or -cultured microtissues are often used in cell transplantation rather than single cells [28,29], it is important to determine whether MES can be used to pattern and organize microtissues directly. Third, as hydrogel materials are quite fragile and hard to handle, we will investigate whether they are suited to fabricate macroencapsulation devices.

To address these questions, we used agarose-based hydrogel membranes to create a model macroencapsulation system. Fabrication of microwell patterns was investigated to test whether high-density arrays of cell spheroids can be generated through a micromolding process. NIH 3T3 fibroblast spheroids, self-assembled from dissociated cells, were used as model microtissues, and seeded directly onto agarose membranes patterned with microwells. The fidelity of these microtissues to the topographical patterns was examined. Following this, we encapsulated cell-spheroidal arrays in sandwiched gel layers. A one-week preliminary experiment was performed to evaluate the stability of the subcutaneously embedded MES. Detailed theoretical analysis was also performed to elucidate the relationship between micropatterns and the transplantation capacity of membrane-based encapsulation. Our study may help to lay foundations for designing a new generation of immunoisolation devices for cell-based therapy.

1 Materials and methods

1.1 Materials and cell culture

Water was distilled and deionized at 18 M resistance (Gelante Pure Water, China). Agarose (type IX-A, ultra-low gelling temperature (ULGT)) was purchased from Sigma-Aldrich (USA). NIH 3T3 fibroblasts were obtained from the Cell Culture Center of the Institute of Basic Medical Sciences (Beijing, China). Human hepatocellular carcinoma HepG2 cells were a kind gift from Dr. Hongkui Deng (College of Life Sciences, Peking University, Beijing, China). All cell culture reagents were purchased from Invitrogen (USA), unless otherwise specified.

Cells were cultured under a humidified atmosphere with 5% CO_2 at 37°C. Cell media were replaced every 2–3 days. HepG2 and NIH 3T3 cells were both maintained in DMEM supplemented with 10% fetal bovine serum and 1% penicillin/streptomycin.

1.2 Generation of microwell-patterned agarose membranes

Silica (Si) wafers were fabricated with microwell patterns of pre-defined feature sizes via standard photolithographic techniques (First MEMS Corp., China). The height of the micropatterns was 80 μm. From these master patterns, complementary polydimethylsiloxane (PDMS) replicas were prepared by curing the PDMS prepolymers (mixed at 10:1 ratio with the crosslinking catalyst Sylgard 184, Dow Corning Corp., USA) over the Si master at 80°C for 2 h; the resulting PDMS molds were peeled off and cut into stamps with 5 mm×5 mm patterned surfaces. The trimmed PDMS molds were further cleaned in a 70% ethanol solution, exposed under UV light for 30 min for sterilization and stored for future use.

To generate micropatterned hydrogel membranes, we dissolved ULGT agarose powder in phosphate-buffered saline (PBS) at 60°C to a concentration of 30 mg mL^{-1}. The resulting pre-gel stock solutions were sonicated for 30 min

to remove bubbles. 180 μL solutions were then pipetted into 48-well plates or 8-well Lab-Tek chamber slides (Nunc, Thermo Fishers, USA) and micromolded by placing PDMS stamps with negative microwell patterns on top of the agarose liquid. The gels were cured overnight at 4°C and the resulting microwell-patterned membranes were used for cell culture.

1.3 Imaging analysis of microwell-patterned agarose membranes

The agarose membranes were characterized by stylus profilometry (Dektak 150 Veeco Metrology, USA) to analyze of the depth of the patterns on the surface. Specifically, a micropatterned membrane on top of a glass slide was placed on the sample stage and the stylus was moved along a selected straight line across the microwell patterns. The step height between the lower bottom and the upper ridge of the well was thus obtained.

Phase-contrast microscopy was conducted to image the agarose membranes with and without cells from the top using an IX71 fluorescence microscope (Olympus, Japan). To obtain the side-view of the microwell pattern, we carefully sliced hydrogel samples prepared in Lab-Tek chamber slides across the microwells into 2-mm-wide strips. The hydrogel strip was then flipped onto its side on a coverslip for image analysis.

1.4 Generation of encapsulated microtissue arrays from dissociated cells or pre-formed multi-cellular spheroids

To seed HepG2 hepatocytes or NIH 3T3 fibroblasts on microwell-patterned membranes, we suspendeded dissociated cells in media at 2×10^5 cell mL^{-1}, and the suspensions were pipetted at 0.4 mL/well onto the microwell-patterned membranes in 48-well plates. Cells were allowed to sediment to the bottom of microwells. After 24 h, the supernatant was then carefully aspirated to remove unattached floating cells and fresh media were added. To generate the sandwiched encapsulation model, we pipetted 20 μL pre-gel agarose solutions onto microwells containing microtissue arrays and allowed to gel at 4°C for 30 min. The hydrogel membrane containing the encapsulated microtissues was maintained for up to 20 d, with medium exchange every other day. The assembled cellular spheroids in the microwells were imaged via phase-contrast microscopy.

To investigate the seeding of pre-formed spheroids, we plated the fibroblast spheroids at 8.0×10^4 cells/well on 24-well ultra-low attachment plates (Corning, USA) and rotated at 160 r min^{-1} for 15 min on an orbital shaker every 30 min for four repeats and then cultured without motion in an incubator for several hours. Once the multi-cellular spheroids were formed, they were collected by centrifugation at RCF 160×*g* for 5 min.

To quantitatively analyze spheroid size and numbers, we resuspended the cellular spheroids in 150 μL culture medium and plated on 96-well plates. Four fields of view (upper left, upper right, lower left and lower right) that cover the whole bottom area of the well under 4× magnification were selected and phase contrast images were recorded. The diameters of the spheroids were determined through measurement of the pixel numbers of lines drawn crossing the spheroids, followed by conversion to actual lengths using ImageJ analysis software (NIH, USA). Spheroid numbers were also counted in each field of view.

To analyze the distribution of spheroids settled within microwells, we seeded spheroids collected from one, two and three wells of ultra-low attachment plates onto different microwell patterns. After 24 h, the microwells were divided into four cornered regions and phase contrast images were recorded at 4× (objective lens) magnification. The four images were pieced together to obtain the full view of the patterned area (5 mm×5 mm).

1.5 Cell viability and functional secretion maintained in agarose-based MES

The spheroid arrays were stained with Hoechst 33342 and propidium iodide (PI) (Sigma-Aldrich, USA) at prescribed time points to detect cell viability/death according to the manufacturer's instructions. Necrosis was determined on the basis of positive PI staining in red color, indicative of loss of membrane integrity.

To evaluate the function of encapsulated microtissues in sandwiched membranes, we examined the secretion of albumin and vascular endothelial growth factor (VEGF) from HepG2 hepatocytes and NIH 3T3 fibroblasts, respectively. Specifically, after HepG2 cells were seeded and encapsulated in the micropatterned membrane, the cell culture medium was collected at prescribed time points for each sample and frozen at −20°C for analysis. Then, 400 μL of fresh medium was added and the protein concentration in the culture medium from the collected samples were measured using commercial albumin (Bethyl Laboratories, USA) and VEGF (Quantikine®, R&D Systems, USA) ELISA kits, following the manufacturer's instructions.

1.6 Subcutaneous implantation of agarose-based MES

All procedures were performed in accordance with the regulations approved by the Institutional Animal Care and Use Committee (IACUC) of the Peking University. Six Sprague-Dawley (SD) rats weighing 290–320 g were housed in separate cages and cared for in compliance with protocols approved by the Animal Ethnics Committee at Peking University. Rats were anaesthetized with an intraperitoneal injection of chloral hydrate (400 mg kg^{-1}). Four 1-cm incisions were prepared (two in the left back; two in the right back), and four subcutaneous pouches (about 8×8 mm) were

created lateral to the incisions, at 2 cm intervals, by gentle blunt dissection with scissors. Sandwiched agarose membranes containing NIH 3T3 fibroblast spheroids, that had been prepared and cultured for 4 d in the Lab-Tek plate *in vitro*, were placed into the pocket. Four disks, one over each hip and shoulder, were placed in each rat. Incisions were closed with sutures and the animals were observed until recovery and housed for prescribed time. Animals were sacrificed 7 d post-implantation by CO_2 asphyxiation.

1.7 Histological analysis

Implants and surrounding tissue were harvested from sacrificed rats, fixed in 4% paraformaldehyde, and dehydrated sequentially in a series of graded ethanol with concentration at 70%–100% before paraffin embedding. The embedded hydrogel-tissue samples were subsequently microtomed into 6-μm-thick sections and stained with hematoxylin and eosin (H&E) via a standard protocol. The histological images were obtained using a BX51 microscope (Olympus) under bright-field mode.

1.8 Quantitative analysis

Statistical comparisons were performed by one-way analysis of variance (ANOVA) followed by the Newman-Keuls test to compare data pairs using SigmaStat 3.5 software (Systat Software Inc., USA), and the difference was considered statistically significant when $P<0.05$. All quantitative results were presented as means±standard deviation (SD).

2 Results

2.1 Generation of high-density microtissue arrays on agarose membranes

The agarose hydrogel membranes patterned with microwell structures were fabricated through a micromolding process using a PDMS stamp. To build the encapsulation model, we dispensed pre-gel solutions to cover the microwells once the cellular spheroid arrays were formed (Figure 1A). We chose hexagonal tiling, the densest way to arrange circles in two dimensions, to create microwells with a diameter of 100 or 200 μm. To vary the density of microwells, we defined the peripheral distance between two neighboring microwells (*d*), as shown in Figure 1B, at either 1/2 or 1/4 of the microwell radius (*r*).

All four types of microwell patterns were successfully created and the resulting hydrogel membranes could be removed from the container that initially held the gel solution (Figure 2A). From the side-view, the whole thickness of the membranes was measured at 204.25±46.54 μm (n=8) (Figure 2B). The characterization by contact profilometry tech-

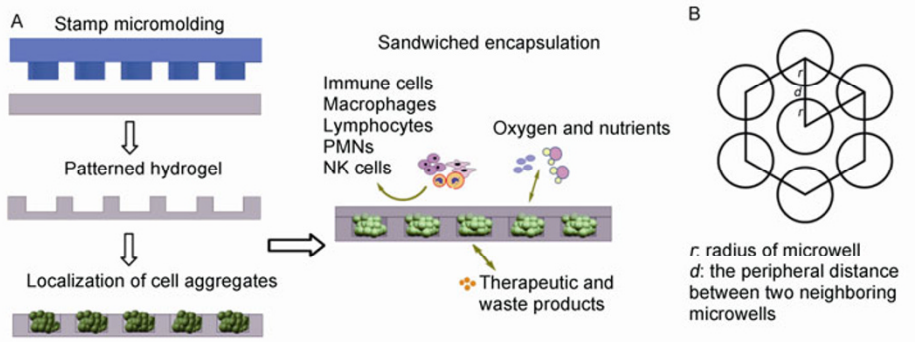

Figure 1 A, Schematic fabrication of micropatterned membranes and sandwiched encapsulation system. B, Schematic illustration of the dense hexagonal arrangement of the circular microwells.

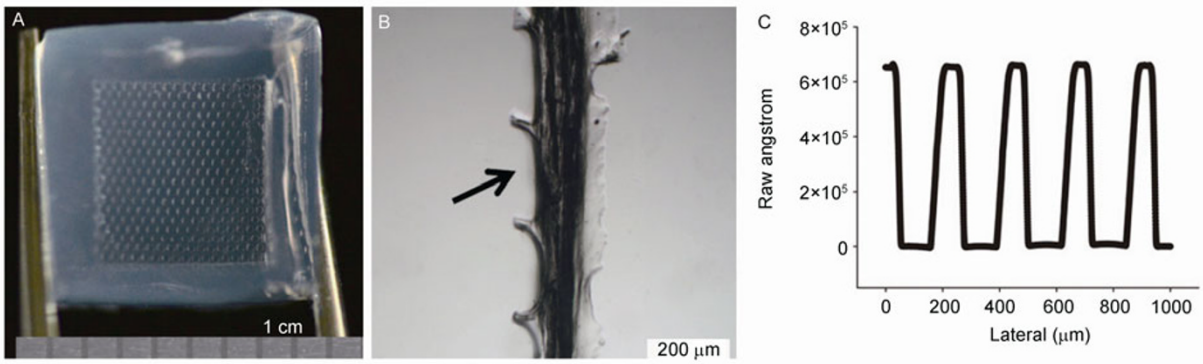

Figure 2 A, Agarose membranes with microwell patterns. B, The side-view of a micropatterned agarose membrane, with the arrow indicating the surface of the microwells. C, Profilometric characterization of the microwell depths.

niques indicated that the depth of microwells was 61.3± 4.1 μm (n=3) (Figure 2C).

When dissociated single cells, either HepG2 hepatocytes or NIH 3T3 fibroblasts, were seeded into microwells, they were found to settle at the bottom of the microwells. The process occurred within a few minutes and the percentage of microwells filled with cells generally reached 80%–90% at 24 h (Figure 3 and Table 1). The average diameter of spheroids increased with the size of microwells. From the statistical results of both 100-μm and 200-μm microwells, it is noted that the HepG2 spheroids tend to be smaller in microwells of higher density (Table 1).

2.2 Direct seeding of pre-assembled cellular spheroids onto agarose microwells

Both HepG2 hepatocytes and NIH 3T3 fibroblasts formed 3-D multicellular aggregates on ultra-low attachment plates. However, the aggregation of HepG2 hepatocytes resulted in irregular shapes (Figure S1 in Supporting Information), while NIH 3T3 fibroblast aggregates were obtainable with spheroidal shape. The typical diameter of these fibroblasts spheroids was in the range of 30–100 μm, with the peak value at 40–50 μm (Figure 4). The spheroids were then used as microtissues and directly plated into different types of microwells.

Specially, to seed fibroblast microtissues, we varied the spheroid/microwell ratio (S/M ratio) from 0.35 to 1.15 and 1 to 4 for 100-μm and 200-μm microwells, respectively. Like dissociated cells, the fibroblast spheroids were captured by microwells within a few minutes following seeding (Figure 5A and B). While most of the 100-μm microwells contained no more than one microtissue, many 200-μm microwells captured two or more spheroids (Figure 5C and D). The percentage of microwells containing microtissues increased with the number of initially plated spheroids until the majority of microwells were filled (Figure 6A). When comparing microwells of different sizes, the S/M ratio needed to reach 1.1 and 2.1 for 100-μm and 200-μm microwells, respectively, to have over 80% containing spheroids. The distance between microwells did not have significant impact on the microwell filling ratio. In addition, a very high level of fidelity of the spheroids was observed as can be seen in the trend in Figure 6B, which indicat es that about 70%–80% of the initially seeded spheroids were generally located in microwells.

Table 1 Different types of microwells and formation of multi-cellular spheroids at 24 h

Designated sample name	Microwell diameter (μm)	SD (μm)	Percentage of microwells filled with spheroids (%)	Average diameter of spheroids (μm)
100-A	100	25	89±7.1	62.8±8.8
100-B	100	12.5	78.2±7.8	49.5±8.7
200-A	200	50	90.9±5.0	108.6±13.2
200-B	200	25	88.7±2.6	87.2±8.2

2.3 Viability and function of cells encapsulated in sandwiched membranes

After adding the overlayer of gel solution onto the top of the agarose membrane, cell spheroids formed from single cells

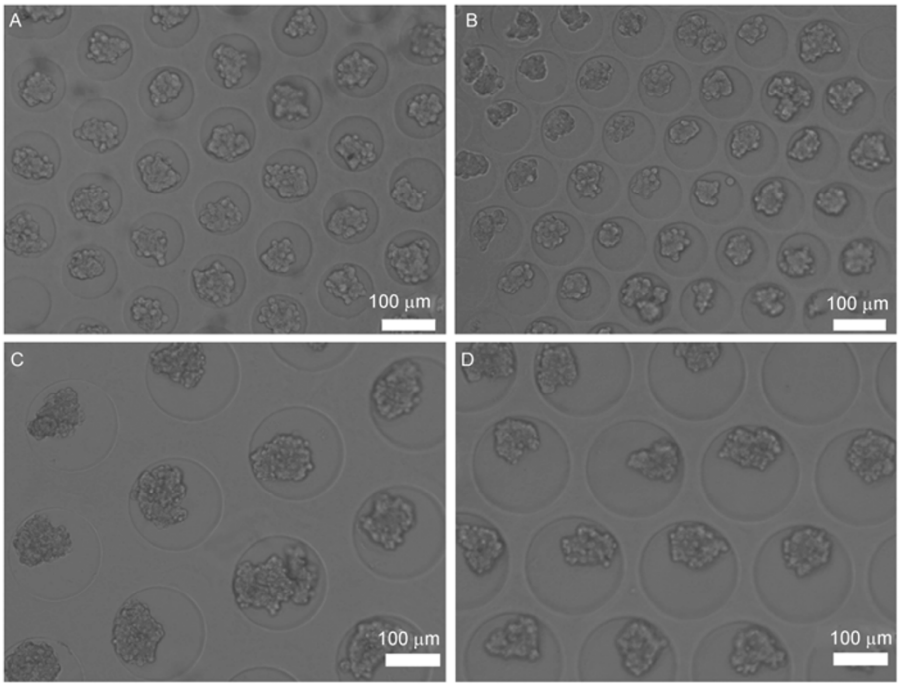

Figure 3 Dissociated HepG2 cells self-assembled into spheroids in different types of microwells. A, B, C and D correspond to the 100-A, 100-B, 200-A and 200-B membranes as listed in Table 1, respectively.

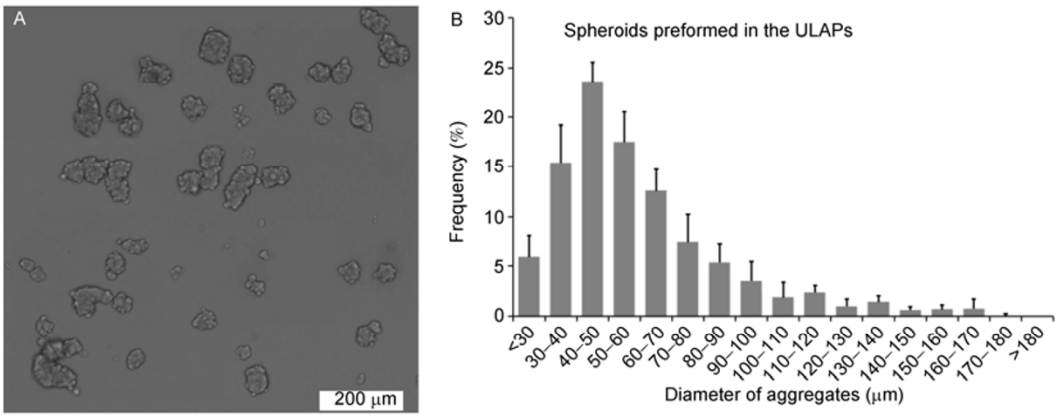

Figure 4 Aggregation of fibroblast cells on ultra-low attachment microplates and the size distribution of the resulting multi-cellular spheroids.

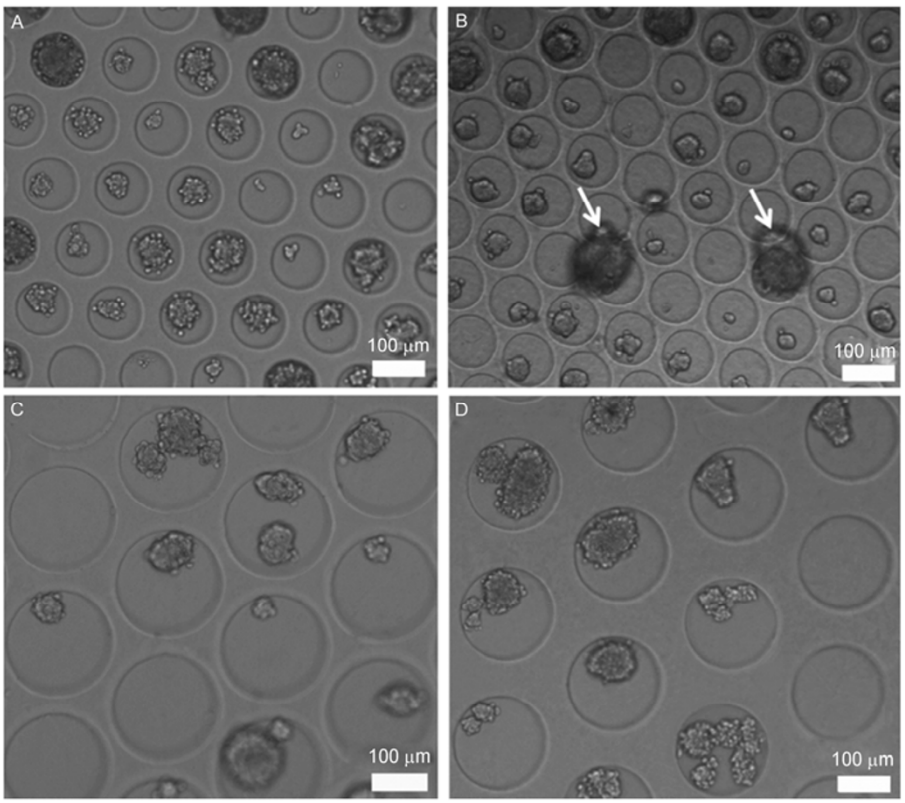

Figure 5 Preformed NIH 3T3 fibroblast spheroids spontaneously located in the microwells at 24 h (S/M ratio: 1~1.2). A, B, C and D correspond to the 100-A, 100-B, 200-A and 200-B membranes, respectively. The white arrows in B indicate floating spheroids in the supernatant.

in microwells were maintained in the sandwiched membranes for up to 3 weeks. As shown in Figure 7, with prolonged cell culture, the Hoechst 33342/PI assay showed few necrotic cells. Unlike the cells in the early period of culture, the cells appeared to fuse together with prolonged culture time, as cell membranes or individual cells became indistinguishable.

The paracrine secretion of albumin and VEGF from HepG2 hepatocyte and NIH 3T3 fibroblast spheroids, respectively, were monitored over a 2-week period (Figure 8). During this time, the paracrine secretion of both types of spheroids increased in the first week and then maintained a steady level. Although the encapsulated cells showed a lower level of secretion at some time points, the production rate/quantity of albumin and VEGF by spheroids with or without the encapsulating layer was generally comparable.

2.4 Subcutaneous encapsulation

To investigate the suitability of hydrogel membranes for

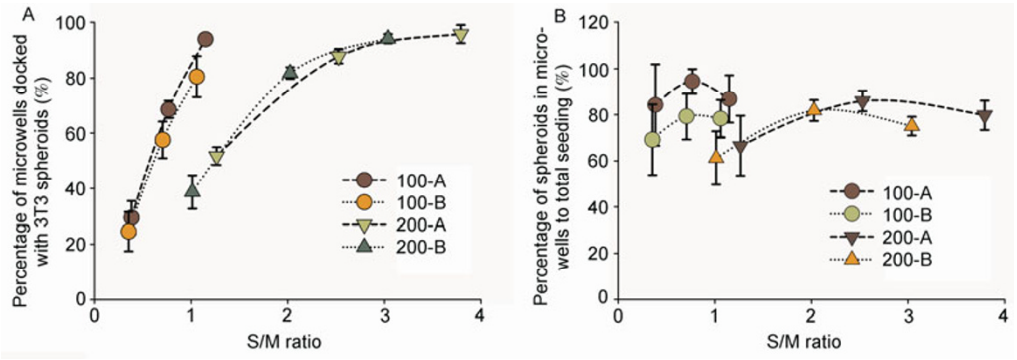

Figure 6 Statistical profiling of fibroblast spheroids captured by different micropatterned membranes. A, The percentage of microwells containing fibroblast spheroids. B, The percentage of spheroids captured by microwells versus the total seeded spheroids (n=3).

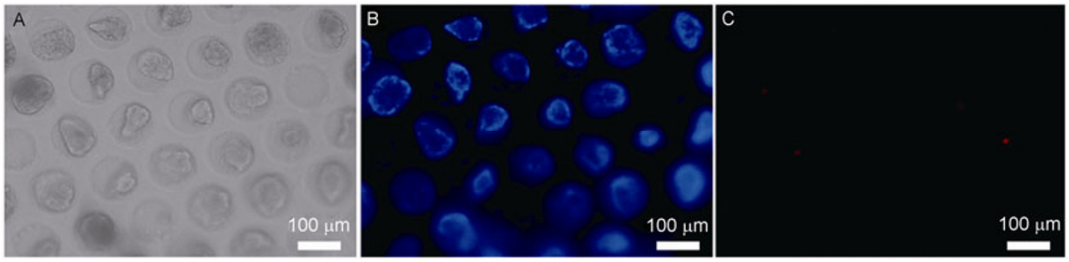

Figure 7 A, Phase contrast image of the spheroids encapsulated in agarose-based MES at 22 d. B, Nuclei of all viable cells stained with the Hoechst 33342 dye are shown in blue. C, Necrotic cells stained with propidium iodide are shown in red.

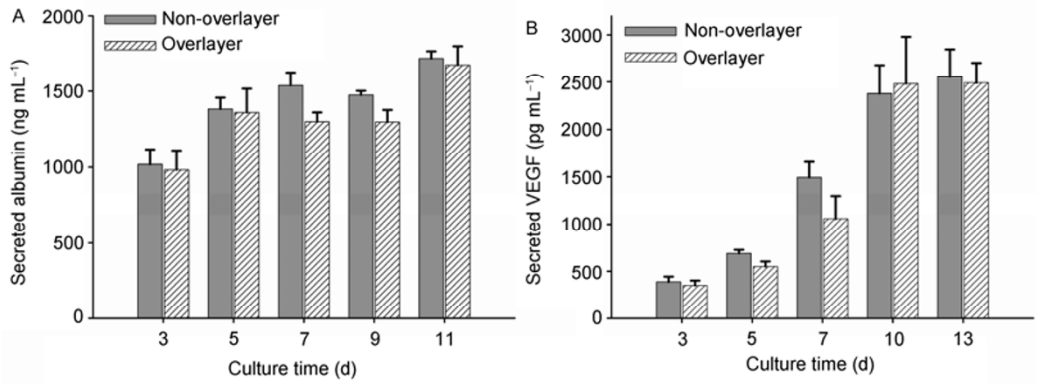

Figure 8 Albumin secretion by HepG2 hepatocyte spheroids (n=5) (A) and VEGF secretion by NIH 3T3 fibroblast spheroids (n=4) (B) in the microwells with or without the encapsulating layer.

transplantation applications, we embedded the encapsulating membranes with a total thickness about 0.5 mm in the subcutaneous tissue of a rat model (Figure 9A). When the tissue was opened up one week later, the macroencapsulation membrane was found to have remained at the implantation site; however, it was surrounded by connective tissue (Figure 9B). By histology analysis, microwell pattern containing cells were observed. It is hard to judge whether the cells remaining in the micropatterns were implanted cells or infiltrated ones from the host tissue (Figure 9C). Some degree of foreign-body response was observed at the periphery of the implanted encapsulation system. (Figure 9D).

3 Discussion

Current macroencapsulation devices are mainly made of planar or tubular membranes with the capacity to isolate cells from the attack of the host immune system. For example, TheraCyte™ devices encapsulate cells/tissues in sealed polytetrafluoroethylene (PTFE)-based membranes [30,31]; islets were also encapsulated in stainless steel mesh tubes with an interior PTFE rod [32]. In these devices, the spatial distribution of microtissues is random, uncontrollable and therefore unable to maintain the microtissues separated when closely packed together. Macroencapsulation devices

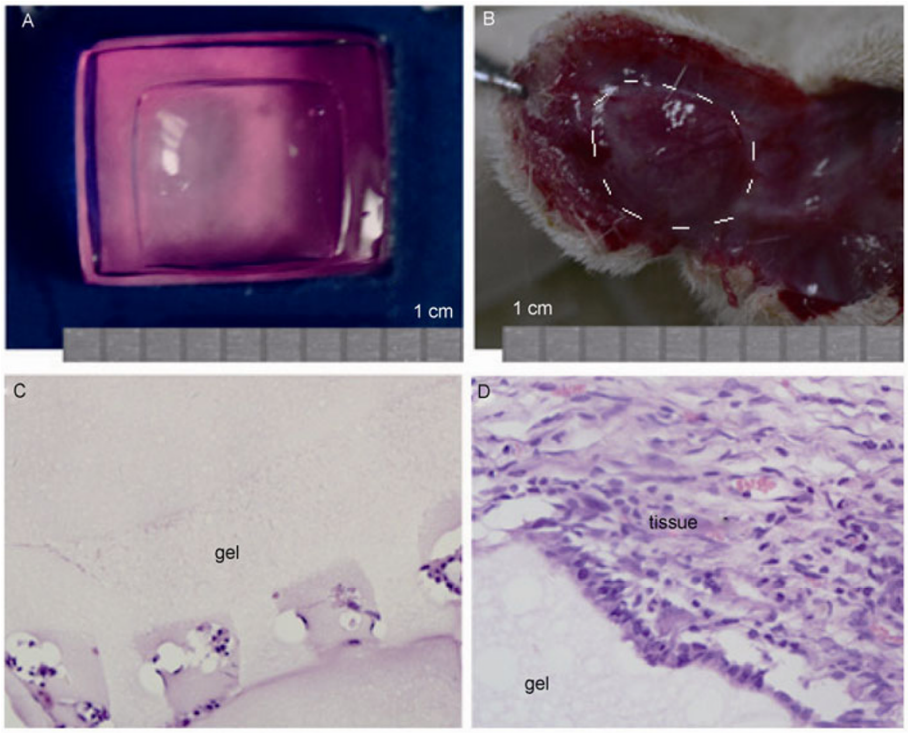

Figure 9 A, Sandwiched agarose membranes containing NIH 3T3 fibroblast spheroids. B, Implanted membranes (in the area circled by white broken lines) 7 d post-implantation. C, H&E stained section containing micropatterned regions. D, H&E stained sections showing the interface between the device and the host tissue.

featured with microstructural patterns ushered in the concept of generating cellular organization at the microscale level. The design may be able to minimize the transplantation volume, increase the encapsulation efficiency and improve the cell viability. Understanding the packing theory of microtissues in MES is therefore a prerequisite for establishing key design principles for this new type of device.

The device with patterned microwells is essentially a 2-D system. If the microwells were arranged through hexagonal close-packing, the percentage area of the microwells ($A_{\text{microwell}}\%$) on the membrane varies with the radius (r) of and the peripheral distance (d) between microwells. Figure 10A draws the trend of $A_{\text{microwell}}\%$ with a normalized parameter, d/r. When d is 1/4 or 1/2 of r, as in the membranes created in this study, $A_{\text{microwell}}\%$ is 71.7% and 58%, respectively. By contrast, we can also monitor the percentage volume of the microwells ($V_{\text{microwell}}\%$) when the spatial feature of the microwell and thickness (t) of the device is varied (Figure 10B). In a typical MES, where d and r are 25 μm and 100 μm, respectively, the total volume of the device could be no more than two- or three-fold the volume of the spheroidal microtissues. Figure 10C shows a chart from which the number of microwells can be obtained given the device geometry. It can be seen that within a 10 cm × 10 cm device, there could be 9.1×10^5 or 2.3×10^5 microwells with a diameter of 100 μm or 200 μm (d/r = 1/2), respectively. The number matches the total islet cell number required for clinical transplantation [15,33–35]. The detailed calculation formulas for theoretical analysis are shown in Figure S2 in Supporting Information.

The above analysis of microwell packing is theoretical. In reality, the generation of substrates with a high-density of microwell arrays may be limited by the mechanical strength of the materials as well as the micromolding process itself. In our study, we found that the microwells could maintain their pre-designed shape even when the distance between microwells was reduced to 12.5 μm. The pattern was also stable after the agarose membrane was immersed in culture medium or transplanted *in vivo*. Further increasing the microwell density could result in defects given the fragility of hydrogel materials.

Stem cell research has grown into an active field in the last two decades and holds great promise to provide revolutionary regenerative treatment for tissue repair [36,37]. Protocols have become available to allow scalable production of stem cells. Moreover, stem cells can be guided in definable ways to differentiate into diverse types of specialized cells. To make these specialized cells functional *in vivo*, new strategies have emerged in recent years to culture 3-D multicellular constructs to promote tissue morphogenesis [38,39]. Given the likelihood that spheroidal microtissues may be harvested from stem cell culture for transplantation, it is important to understand whether the microtissue entities can be manipulated and assembled on substrates or scaf-

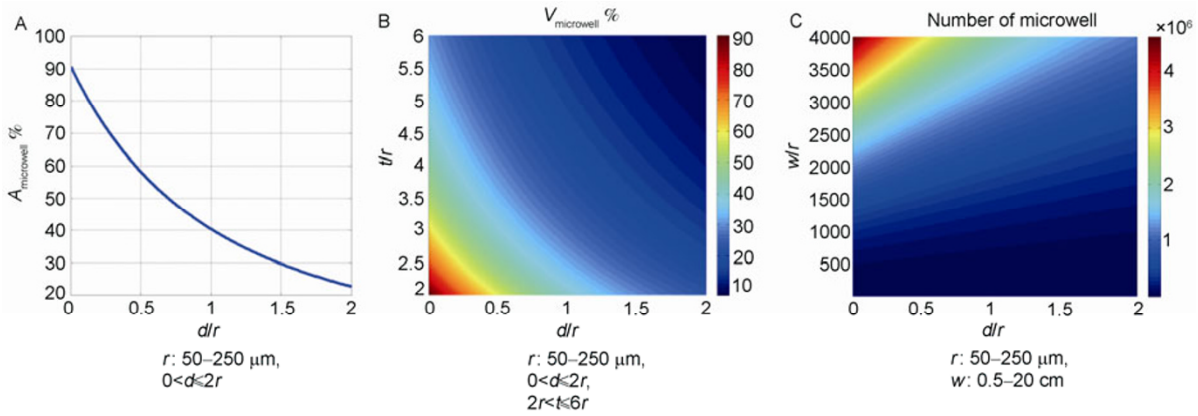

Figure 10 Graphical results showing (A) the percentage area ($A_{microwell}$%), (B) the percentage volume ($V_{microwell}$%) and (C) the number of microwells via hexagonal close-packing in membranes of defined geometrical parameters. *R*, the radius of microwells; *d*, the peripheral distance between microwells; *t*, thickness of the device; *w*, the length of the square device.

folds. When the dissociated cells were seeded into microwells, it was shown that the number of cells trapped in microwells follow a Poisson distribution [40,41]. Microwells could be used to capture single cells and thus study stem cell fate [42]. However, direct seeding of microtissues has not been previously investigated. Herein, we provide evidence that spheroidal microtissues, like the dissociated cells, can be entrapped in microwell structures on the surface of hydrogel membranes. The spheroid distribution patterns vary with the microwell size. We show in our experiments that the distribution of spheroids was more homogeneous on 100-μm microwells than that on 200-μm microwells. The reason could be that the size of spheroids collected from low attachment microplates matched more closely with 100-μm microwells. In contrast, larger microwells may have difficulty in trapping single spheroids in one well and multiple spheroids could aggregate and fill the microwell.

In previous studies, microtissues assembled in microwells with a concave bottom were encapsulated in alginate-based hydrogels and removed from the original mold [25–27]. The resulting encapsulation membranes had one side with arrayed protrusions containing microtissues. Although the membranes enabled dense packing of microtissues, there are problems associated with this method for making devices for clinical application. First, it is hard to achieve complete or controllable encapsulation of microtissues contained in the microwell mold. Separating the hydrogel membranes from the mold may cause damage to the encapsulation microstructures. In addition, the protrusions of the membrane may not represent the optimal surface *in vivo*. In this study, we propose to use sandwiched membranes as a prototype macroencapsulation system. Although the bonding between the bottom and top gel layers may be weak, the fabrication of the device is simple, and allows for the control of membrane thickness and surface features. Our results on the viability and functions of microtissues encapsulated in sandwiched membranes show that the agarose material may afford some level of immunoisolation activity, by allowing sustainable delivery of paracrine factors and the diffusion of oxygen, nutrients and metabolic waste products. However, the *in vivo* study needs further investigation, as the number of cells maintained in the micropattern may well below the implanted cell number. This limitation could be related to the weak mechanical properties of the hydrogel or the imperfect sealing of the two gel layers. In addition, the agarose membrane may not be capable of preventing the permeation of antibodies and complement proteins [43]. Future efforts need to determine a chemistry that bond the two gel layers together and optimize the mechanical and transport properties of immunoisolation materials. Incorporation of extracellular components in encapsulation membranes may also be necessary to promote cell viability and function within the device [26,44].

In conclusion, using an agarose hydrogel model, we investigated key principles relating to designing MES to transplant microtissues with microscale spatial control. Our study shows that high-density microtissue arrays can be generated in micropatterned membranes. The cell density within the device can reach a high level that minimizes the size of the transplantation device. The microwell structures are also effective for directly positioning and organizing microtissue entities, indicating the suitability of the membrane-based devices for manipulating cells at the multicellular level. MES could therefore offer a promising approach for transplanting large quantities of cells/tissues via high-density arrayed patterns. Further development of the macroencapsulation system should be investigated to improve the mechanical stability and biochemical properties of the membrane materials for supporting long-lasting viability of transplanted cells.

This research was financially supported by the Key New Drug Creation and Manufacturing Program (2011ZX09102-010-03) and the National

Natural Science Foundation of China (31170933). We thank Zhou Yan for his assistance with profilometry experiments.

1 Uludag H, De Vos P, Tresco PA. Technology of mammalian cell encapsulation. Adv Drug Deliv Rev, 2000, 42: 29–64
2 Chang TM. Semipermeable Microcapsules. Science, 1964, 146: 524–525
3 Lim F, Sun AM. Microencapsulated islets as bioartificial endocrine pancreas. Science, 1980, 210: 908–910
4 Lee MK, Bae YH. Cell transplantation for endocrine disorders. Adv Drug Deliv Rev, 2000, 42: 103–120
5 Cieslinski DA, David Humes H. Tissue engineering of a bioartificial kidney. Biotechnol Bioeng, 1994, 43: 678–681
6 Chang TM, Hybrid artificial cells: microencapsulation of living cells. ASAIO J 1992, 38: 128–130
7 Emerich DF, Salzberg HC. Update on immunoisolation cell therapy for CNS diseases. Cell Transplant, 2001, 10: 3–24
8 Kin T, Iwata H, Aomatsu Y, Ohyama T, Kanehiro H, Hisanaga M, Nakajima Y. Xenotransplantation of pig islets in diabetic dogs with use of a microcapsule composed of agarose and polystyrene sulfonic acid mixed gel. Pancreas, 2002, 25: 94–100
9 Orive G, Hernandez RM, Rodriguez Gascon A, Calafiore R, Chang TM, de Vos P, Hortelano G, Hunkeler D, Lacik I, Pedraz JL. History, challenges and perspectives of cell microencapsulation. Trends Biotechnol, 2004, 22: 87–92
10 O'Sullivan ES, Vegas A, Anderson DG, Weir GC. Islets transplanted in immunoisolation devices: a review of the progress and the challenges that remain. Endocr Rev, 2011, 32: 827–844
11 Bonner-Weir S, Weir GC. New sources of pancreatic beta-cells. Nat Biotechnol, 2005, 23: 857–861
12 Kroon E, Martinson LA, Kadoya K, Bang AG, Kelly OG, Eliazer S, Young H, Richardson M, Smart NG, Cunningham J, Agulnick AD, D'Amour KA, Carpenter MK, Baetge EE. Pancreatic endoderm derived from human embryonic stem cells generates glucose-responsive insulin-secreting cells in vivo. Nat Biotechnol, 2008, 26: 443–452
13 Liu X, Wang Y, Li Y, Pei X. Research status and prospect of stem cells in the treatment of diabetes mellitus. Sci China Life Sci, 2013, 56: 306–312
14 Nafea EH, Marson A, Poole-Warren LA, Martens PJ. Immunoisolating semi-permeable membranes for cell encapsulation: focus on hydrogels. J Control Release, 2011, 154: 110–122
15 Teramura Y, Iwata H. Bioartificial pancreas microencapsulation and conformal coating of islet of Langerhans. Adv Drug Deliv Rev, 2010, 62: 827–840
16 Lacy PE, Hegre OD, Gerasimidi-Vazeou A, Gentile FT, Dionne KE. Maintenance of normoglycemia in diabetic mice by subcutaneous xenografts of encapsulated islets. Science, 1991, 254: 1782–1784
17 Suzuki K, Bonner-Weir S, Hollister-Lock J, Colton CK, Weir GC. Number and volume of islets transplanted in immunobarrier devices. Cell Transplant, 1998, 7: 47–52
18 Suzuki K, Bonner-Weir S, Trivedi N, Yoon KH, Hollister-Lock J, Colton CK, Weir GC. Function and survival of macroencapsulated syngeneic islets transplanted into streptozocin-diabetic mice. Transplantation, 1998, 66: 21–28
19 Qi M, Gu Y, Sakata N, Kim D, Shirouzu Y, Yamamoto C, Hiura A, Sumi S, Inoue K. PVA hydrogel sheet macroencapsulation for the bioartificial pancreas. Biomaterials, 2004, 25: 5885–5892
20 Lee SH, Hao E, Savinov AY, Geron I, Strongin AY, Itkin-Ansari P. Human beta-cell precursors mature into functional insulin-producing cells in an immunoisolation device: implications for diabetes cell therapies. Transplantation, 2009, 87: 983–991
21 Hwang YS, Chung BG, Ortmann D, Hattori N, Moeller HC, Khademhosseini A. Microwell-mediated control of embryoid body size regulates embryonic stem cell fate via differential expression of WNT5a and WNT11. Proc Natl Acad Sci USA, 2009, 106: 16978–16983
22 Wong SF, No daY, Choi YY, Kim DS, Chung BG, Lee SH. Concave microwell based size-controllable hepatosphere as a three-dimensional liver tissue model. Biomaterials, 2011, 32 : 8087–8096
23 Bernard AB, Lin CC, Anseth KS. A microwell cell culture platform for the aggregation of pancreatic beta-cells. Tissue Eng Part C, Methods, 2012, 18: 583–592
24 Jiang LY, Luo Y. Guided assembly of endothelial cells on hydrogel matrices patterned with microgrooves: a basic model for microvessel engineering. Soft Matter, 2013, 9: 1113–1121
25 Rago AP, Chai PR, Morgan JR. Encapsulated arrays of self-assembled microtissues: an alternative to spherical microcapsules. Tissue Eng Part A, 2009, 15: 387–395
26 Lee KH, No da Y, Kim SH, Ryoo JH, Wong SF, Lee SH. Diffusion-mediated in situ alginate encapsulation of cell spheroids using microscale concave well and nanoporous membrane. Lab on a chip, 2011, 11: 1168–1173
27 Lee BR, Hwang JW, Choi YY, Wong SF, Hwang YH, Lee DY, Lee SH. In situ formation and collagen-alginate composite encapsulation of pancreatic islet spheroids. Biomaterials, 2012, 33: 837–845
28 Wang T, Lacik I, Brissova M, Anilkumar AV, Prokop A, Hunkeler D, Green R, Shahrokhi K, Powers AC. An encapsulation system for the immunoisolation of pancreatic islets. Nat Biotechnol, 1997, 15: 358–362
29 Wilson JT, Chaikof EL. Challenges and emerging technologies in the immunoisolation of cells and tissues. Adv Drug Deliv Rev 2008, 60: 124–145
30 Sorenby A, Rafael E, Tibell A, Wernerson A. Improved histological evaluation of vascularity around an immunoisolation device by correlating number of vascular profiles to glucose exchange. Cell Transplant, 2004, 13: 713–719
31 Sorenby AK, Kumagai-Braesch M, Sharma A, Hultenby KR, Wernerson AM, Tibell AB. Preimplantation of an immunoprotective device can lower the curative dose of islets to that of free islet transplantation: studies in a rodent model. Transplantation, 2008, 86: 364–366
32 Valdes-Gonzalez RA, Dorantes LM, Garibay GN, Bracho-Blanchet E, Mendez AJ, Davila-Perez R, Elliott RB, Teran L, White DJ. Xenotransplantation of porcine neonatal islets of Langerhans and Sertoli cells: a 4-year study. Eur J Endocrinol, 2005, 153: 419–427
33 Ryan EA, Paty BW, Senior PA, Bigam D, Alfadhli E, Kneteman NM, Lakey JR, Shapiro AM. Five-year follow-up after clinical islet transplantation. Diabetes, 2005, 54: 2060–2069
34 Shapiro AM, Ricordi C, Hering BJ, Auchincloss H, Lindblad R, Robertson RP, Secchi A, Brendel MD, Berney T, Brennan DC, Cagliero E, Alejandro R, Ryan EA, DiMercurio B, Morel P, Polonsky KS, Reems JA, Bretzel RG, Bertuzzi F, Froud T, Kandaswamy R, Sutherland DE, Eisenbarth G, Segal M, Preiksaitis J, Korbutt GS, Barton FB, Viviano L, Seyfert-Margolis V, Bluestone J, Lakey JR. International trial of the Edmonton protocol for islet transplantation. N Engl J Med, 2006, 355: 1318–30
35 Hatziavramidis DT, Karatzas TM, Chrousos GP. Pancreatic islet cell transplantation: an update. Ann Biomed Eng, 2013, 41: 469–76
36 Takahashi K, Tanabe K, Ohnuki M, Narita M, Ichisaka T, Tomoda K, Yamanaka S. Induction of pluripotent stem cells from adult human fibroblasts by defined factors. Cell, 2007, 131: 861–872
37 Baraniak PR, McDevitt TC. Stem cell paracrine actions and tissue regeneration. Regen Med, 2010, 5: 121–143
38 Ruiz SA, Chen CS. Emergence of patterned stem cell differentiation within multicellular structures. Stem Cells, 2008, 26: 2921–2927
39 Lin RZ, Chang HY. Recent advances in three-dimensional multicellular spheroid culture for biomedical research. Biotechnol J, 2008, 3: 1172–1184
40 Ino K, Okochi M, Konishi N, Nakatochi M, Imai R, Shikida M, Ito A, Honda H. Cell culture arrays using magnetic force-based cell patterning for dynamic single cell analysis. Lab on a chip, 2008, 8: 134–142
41 Charnley M, Textor M, Khademhosseini A, Lutolf MP. Integration column: microwell arrays for mammalian cell culture. Integr Biol (Camb), 2009, 1: 625–634
42 Gobaa S, Hoehnel S, Roccio M, Negro A, Kobel S, Lutolf MP. Artificial niche microarrays for probing single stem cell fate in high

throughput. Nat Methods. 2011, 8: 949–55
43 Iwata H, Murakami Y, Ikada Y. Control of complement activities for immunoisolation. Ann N Y Acad Sci, 1999, 875: 7–23
44 Steele JA, Barron AE, Carmona E, Halle JP, Neufeld RJ. Encapsulation of protein microfiber networks supporting pancreatic islets. J Biomed Mater Res A, 2012, 100: 3384–3391

Supporting Information

Figure S1 HepG2 hepatocyte aggregates in irregular shapes on ultra-low attachment microplates.

Figure S2 Formula for calculating (A) the percentage area, (B) the percentage volume, and (C) the number of microwells in membranes of defined geometrical parameters.

The supporting information is available online at life.scichina.com and link.springer.com. The supporting materials are published as submitted, without typesetting or editing. The responsibility for scientific accuracy and content remains entirely with the authors.